



CHORUS

This is the accepted manuscript made available via CHORUS. The article has been published as:

Raman scattering study of $\text{NaFe}_{0.53}\text{Cu}_{0.47}\text{As}$

W.-L. Zhang, Y. Song, W.-Y. Wang, C.-D. Cao, P.-C. Dai, C.-Q. Jin, and G. Blumberg

Phys. Rev. B **98**, 094512 — Published 13 September 2018

DOI: [10.1103/PhysRevB.98.094512](https://doi.org/10.1103/PhysRevB.98.094512)

Raman scattering study of NaFe_{0.53}Cu_{0.47}As

W.-L. Zhang,^{1,*} Y. Song,² W.-Y. Wang,² C.-D. Cao,^{2,†} P.-C. Dai,² C.-Q. Jin,^{3,4} and G. Blumberg^{1,5,‡}

¹Department of Physics & Astronomy, Rutgers University, Piscataway, New Jersey 08854, USA

²Department of Physics and Astronomy and Rice Center for Quantum Materials, Rice University, Houston, Texas 77005, USA

³Beijing National Laboratory for Condensed Matter Physics and Institute of Physics, Chinese Academy of Sciences, Beijing 100190, China

⁴Collaborative Innovation Center of Quantum Matter, Beijing, China

⁵National Institute of Chemical Physics and Biophysics, Akadeemia tee 23, 12618 Tallinn, Estonia

(Dated: August 27, 2018)

We use polarization-resolved Raman scattering to study lattice dynamics in NaFe_{0.53}Cu_{0.47}As single crystal. We identify 4 A_{1g} phonon modes at 126, 172, 183 and 197 cm^{-1} , and 4 B_{3g} phonon modes at 101, 139, 173, 226 cm^{-1} (D_{4h} point group). The phonon spectra are consistent with the $Ibam$ space group, which confirms that the Cu and Fe atoms form a stripe order. The temperature dependence of the phonon spectra suggests weak electron-phonon and magneto-elastic interactions.

The parent compound of iron-pnictide superconductor, NaFeAs, is a “bad metal”. It exhibits a tetragonal to orthorhombic transition at 52 K, a paramagnetic to spin-density wave (SDW) transition at 41 K, and a superconducting transition at 23 K [1]. Doping copper into NaFeAs suppresses both the orthorhombic and SDW orders and enhances superconductivity [2–4]. Recently, it was shown that heavy Cu substitution on the Fe site induces Mott-insulator-like behavior [5, 6]. The electronic properties of the heavily doped NaFe_{1-x}Cu_xAs are similar to lightly doped cuprates [5, 7, 8].

For Cu substitution concentration $x > 0.44$ a long-range collinear antiferromagnetic (AFM) order with magnetic moments residing only on the Fe sites develops below 200 K. The moment increases with Cu concentration substitution x [6]. At the solubility limit near $x = 0.5$, new superlattice peaks appear in the TEM diffraction pattern, which are interpreted as the signature of Cu and Fe stripe order formation [6], as depicted in inset of Fig. 1. Compared to the parent NaFeAs compound in the tetragonal phase, the stripe-ordering of Cu and Fe in heavily-doped NaFe_{1-x}Cu_xAs removes the lattice four-fold rotational symmetry and reduces the crystallographic space group from $Fm\bar{3}m$ (point group D_{4h}) to $Ibam$ (point group D_{2h}), making a structural analogue of the magnetic order in parent NaFeAs crystals.

Here we present polarization-resolved Raman scattering study of the lattice dynamics for NaFe_{0.53}Cu_{0.47}As single crystals. Four A_g phonon modes at 126, 172, 183 and 197 cm^{-1} and four B_{3g} phonon modes at 101, 139, 173, 226 cm^{-1} are identified. The phonon spectra are consistent with the Fe/Cu stripe-ordered structure. All the observed phonons exhibit symmetric line shape. Across the AFM phase transition, no phonon anomaly is observed. The data suggests weak electron-phonon and magneto-elastic interaction.

NaFe_{1-x}Cu_xAs single crystals were grown by self-flux method [6, 9]. The nominal Cu concentration was $x = 0.85$, which resulted in $x = 0.47$ actual concentration [6]. The preparation of the reference LiFeAs single crystal is

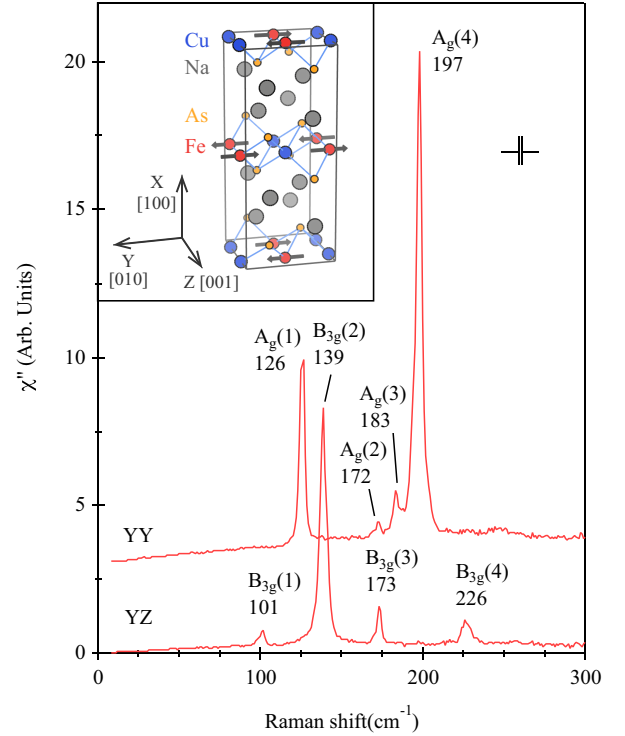


FIG. 1. Raman scattering spectra of NaFe_{0.53}Cu_{0.47}As crystal for YY+ZZ and YZ+ZY scattering geometries at 250 K measured with 1.9 eV excitation. The spectral resolution is 2.5 cm^{-1} . Inset: NaFe_{0.5}Cu_{0.5}As unit cell with Cu and Fe collinear stripe order. Arrows on the Fe sites mark the magnetic moments.

described in [10].

The NaFe_{1-x}Cu_xAs crystal belongs to $Ibam$ space group at room temperature, as shown in the inset of Fig. 1. The crystallographic principle axis [001] of the $Ibam$ group is along Fe(Cu) stripe direction. We define X, Y and Z axes along crystallographic [100], [010] and [001] axes and Y'/Z' along [011]/[0 $\bar{1}$ 1] directions (inset Fig. 2(a)).

There are 12 atoms in the primitive unit cell. Group

TABLE I. Phonon mode decomposition at the Γ point and selection rules for Raman-active modes in $Ibam$ space group.

		Irreducible representations
Acoustic		$B_{1u}+B_{2u}+B_{3u}$
IR		$3B_{1u}+5B_{2u}+5B_{3u}$
Raman		$4A_g+6B_{1g}+4B_{2g}+4B_{3g}$
Silent		$2A_u$
Atom	Wyckoff position	Raman active modes
Na	8j	$2A_g+2B_{1g}+B_{2g}+B_{3g}$
Fe	4b	$B_{1g}+B_{2g}+B_{3g}$
Cu	4a	$B_{1g}+B_{2g}+B_{3g}$
As	8j	$2A_g+2B_{1g}+B_{2g}+B_{3g}$

theoretical analysis infers $4A_g + 6B_{1g} + 4B_{2g} + 4B_{3g} + 2A_u + 4B_{1u} + 6B_{2u} + 6B_{3u}$ [11] symmetry decomposition of the 36 phonon modes at the Brillouin center Γ point. All the even g modes are Raman active. The irreducible representations and decomposition of the Raman active modes by symmetry are summarized in Table I.

Polarization resolved low temperature Raman scattering measurements were performed in a quasi-back scattering setup from natural cleaved (100) surface [12]. Polarizers with better than 1:500 extinction ratio were employed [13]. Samples were cleaved in nitrogen-filled glove bag and immediately transferred to continuous helium gas flow optical cryostat. We used 1.9 and 2.6 eV excitations from Kr^+ laser, where the laser was focused into a $50 \times 50 \mu m^2$ spot on the sample. The power was kept below 10 mW to minimize the laser heating. The local laser heating was estimated [14, 15] and kept at less than 5 K. All referred temperatures are corrected for the laser heating.

The Raman scattering signal was analyzed by a triple-stage spectrometer with the spectral resolution setting at about 2 cm^{-1} . We used scattering geometries $\mu\nu$ with $\mu/\nu = Y, Z, Y'$ and Z' , where $\mu\nu$ is short for $\bar{X}(\mu\nu)X$ in Porto's notation. All spectra were corrected for the spectral response to obtain the Raman scattering intensity $I_{\mu\nu}(\omega, T)$. The Raman susceptibility $\chi''_{\mu\nu}(\omega, T)$ was related to $I_{\mu\nu}(\omega, T)$ by $I_{\mu\nu}(\omega, T) = \chi''_{\mu\nu}(\omega, T)[1 + n(\omega, T)]$, where $n(\omega, T)$ is the Bose factor.

In Table II we list the Raman tensor for D_{2h} group and the selection rule for experimentally accessible polarizations [16]. Due to twin structure [6], the collected signal from (100) surface is a superposition of Raman scattering intensities from two types of orthogonal domains. For example, the signal for parallel polarized scattering geometry along the crystallographic axes contains the intensity from YY geometry for one type of domain and ZZ geometry for the other type of domain. We denote this scattering geometry as YY+ZZ. Similarly, cross polarized signal along the crystallographic axes contains contributions from YZ and ZY geometries, is denoted YZ+ZY,

and cross polarized signal along the diagonal directions contains contributions from $Y'Z'$ and $Z'Y'$ scattering geometries, is denoted $Y'Z'+Z'Y'$.

Following notations of Table II, we assign all phonons that appear in the YY+ZZ geometry to the A_g symmetry modes, and those appear in the YZ+ZY geometry to the B_{3g} modes.

In Fig. 1 we show the Raman response for $NaFe_{0.53}Cu_{0.47}As$ crystal at 250 K for YY+ZZ and YZ+ZY scattering geometries. We identify all the A_g and B_{3g} phonon modes predicted by group theory: four A_g symmetry modes at 126, 172, 183 and 197 cm^{-1} , and four B_{3g} symmetry modes at 101, 139, 173, and 226 cm^{-1} . All modes show symmetric line shape.

We note that at the same frequency as the A_g phonon modes, some modes with weaker intensity are also observed for the $Y'Z'+Z'Y'$ geometry for both 2.6 eV and 1.9 eV laser excitations (Figs. 2(a)-(c)). The intensity of the *leaking* modes is about 10% of the A_g phonon intensity in the YY+ZZ geometry, which is much higher than the experimental polarization extinction ratio. In Fig. 2(d) we show data for LiFeAs tetragonal structure [17] measured by employing same setup. If the substituted Cu ions on Fe sites would be randomly disordered, the $NaFe_{1-x}Cu_xAs$ structure would have same point group symmetry as the LiFeAs structure. By symmetry, no Raman active phonon are allowed in the XY scattering geometry for LiFeAs structure. As we demonstrate in the inset of Fig. 2(d), the *leakage* intensity for tetragonal LiFeAs structure is less than a percent.

Based on the Raman scattering selection rules, we can deduct that the *leakage* intensity is proportional to

TABLE II. Raman tensor and selection rules for Raman-active modes in D_{2h} group.

		$R_{A_g} = \begin{bmatrix} a & 0 & 0 \\ 0 & b & 0 \\ 0 & 0 & c \end{bmatrix}$	$R_{B_{1g}} = \begin{bmatrix} 0 & d & 0 \\ e & 0 & 0 \\ 0 & 0 & 0 \end{bmatrix}$
		$R_{B_{2g}} = \begin{bmatrix} 0 & 0 & f \\ 0 & 0 & 0 \\ g & 0 & 0 \end{bmatrix}$	$R_{B_{3g}} = \begin{bmatrix} 0 & 0 & 0 \\ 0 & 0 & h \\ 0 & i & 0 \end{bmatrix}$
(001) surface	XX	YY	XY/YX
A_g	a^2	b^2	0
B_{1g}	0	0	d^2/e^2
(010) surface	XX	ZZ	XZ/ZX
A_g	a^2	c^2	0
B_{2g}	0	0	f^2/g^2
(100) surface	YY/ZZ	YZ/ZY	$Y'Y'/Z'Z'$ $Y'Z'/Z'Y'$
A_g	b^2/c^2	0	$(b+c)^2/4$ $(b-c)^2/4$
B_{3g}	0	h^2/i^2	$(h+i)^2/4$ $(h-i)^2/4$

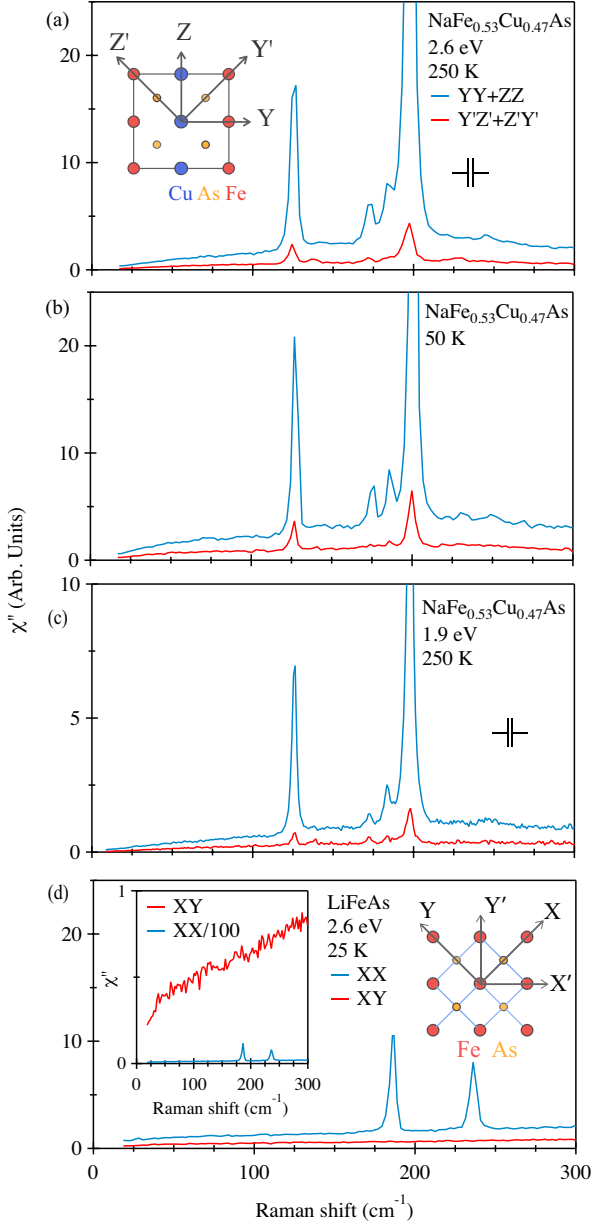


FIG. 2. (a)-(b) A_g -symmetry Raman active phonon modes measured from $\text{NaFe}_{0.53}\text{Cu}_{0.47}\text{As}$ crystal at (a) 250 and (b) 50 K in $YY+ZZ$ (blue) and $Y'Z'+Z'Y'$ (red) scattering geometries with 2.6 eV laser excitation with spectral resolution 3.5 cm^{-1} . (c) Same A_g phonon modes measured at 250 K with 1.9 eV excitation. Inset in (a): top view of the Fe-Cu-As layer for $\text{NaFe}_{0.53}\text{Cu}_{0.47}\text{As}$ structure and the $YZ-Y'Z'$ coordinates. (d) Raman spectra from tetragonal LiFeAs crystal at 25 K measured in $X'X'$ (blue) and XY (red) scattering geometries with 2.6 eV laser excitation. Inset in (d): Left: zoom in of the data where signal for $X'X'$ polarization is divided by 100 to demonstrate lack of detectable *leakage* into cross polarization; and right: top view of the Fe-As layer for LiFeAs crystal structure and the $XY-X'Y'$ coordinates.

$(b-c)^2/4$ (Table I), which is a measure of anisotropic electronic properties between Y and Z directions [15]. The

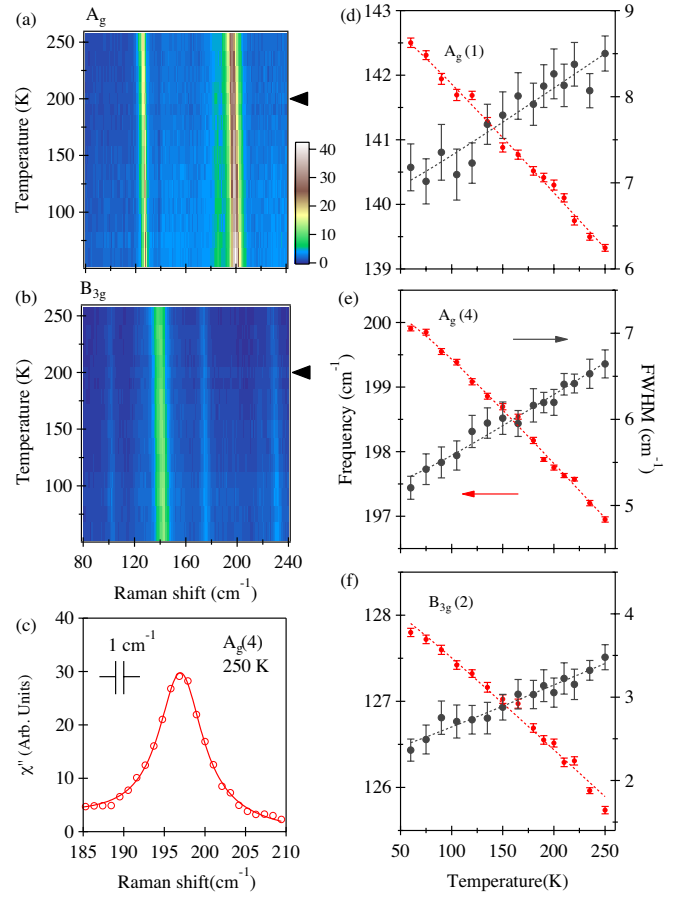


FIG. 3. For $\text{NaFe}_{0.53}\text{Cu}_{0.47}\text{As}$ crystal, temperature dependence of the Raman response in (a) A_g and (b) B_{3g} symmetry channels measured with 1.9 eV laser excitation. The spectral resolution is 1 cm^{-1} . Black arrows indicate the magnetic phase transition at 200 K. (c) Lorentz fit to the $A_g(4)$ phonon at 250 K. Inset shows the spectral resolution. (d)-(f) Temperature dependence of the phonon peak frequency for the $A_g(1)$, $A_g(4)$ and $B_{3g}(2)$ modes. Vertical error bars are one standard deviation error of the Lorentzian fit. The dashed lines show fits of the phonon frequency and linewidth to Eqs. 1-2.

observation of the *leakage* is consistent with suggested formation of a long range stripe order which breaks the crystallographic four-fold symmetry [6]. The count of observed Raman active phonons for $\text{NaFe}_{1-x}\text{Cu}_x\text{As}$ structure also suggests that the size of its primitive cell is four times larger than for NaFeAs structure (Table I), therefore, the only possible consistent structure is the Fe-Cu stripe order phase, as shown in inset of the Fig. 1.

In Figs. 3(a)-(b) we show the intensity plot of the Raman response $\chi''(\omega, T)$ for A_g ($YY+ZZ$) and B_{3g} ($YZ+ZY$) symmetry channels between 250 and 60 K. All phonons show symmetric line shape. The number of the phonon modes and their line shapes do not change across the AFM phase transition at 200 K, suggesting weak magneto-elastic interaction.

We analyze $A_g(1)$, $A_g(4)$ and $B_{3g}(2)$ phonons by fitting

TABLE III. Fitting parameters for the frequency and linewidth of the $A_g(1)$, $A_g(4)$ and $B_{3g}(2)$ modes. The units are in cm^{-1} .

mode	ω_0	ω_1	$2\Gamma_0$	$2\Gamma_1$
$A_g(1)$	128.72 ± 0.07	0.49 ± 0.02	2.06 ± 0.06	0.23 ± 0.02
$A_g(4)$	201.51 ± 0.06	1.21 ± 0.02	4.67 ± 0.07	0.53 ± 0.03
$B_{3g}(2)$	143.82 ± 0.07	0.87 ± 0.02	6.4 ± 0.1	0.41 ± 0.04

to Lorentzian function. As an example, Fig. 3(c) shows the $A_g(4)$ mode at 250 K and its Lorentzian fit. The fitting results are summarized in Figs. 3(d)-(e). Since the magneto-elastic interaction appears to be undetectable within experimental resolution, we fit the modes temperature dependence by anharmonic decay model for the entire temperature range (250 to 60 K) [18]:

$$\omega(T) = \omega_0 - \omega_1 \left[1 + \frac{2}{e^{\hbar\omega_0/2k_B T} - 1} \right] \quad (1)$$

$$\Gamma(T) = \Gamma_0 + \Gamma_1 \left[1 + \frac{2}{e^{\hbar\omega_0/2k_B T} - 1} \right] \quad (2)$$

The fitting results are summarized in Table III.

In summary, we present polarization-resolved Raman scattering study of $\text{NaFe}_{0.53}\text{Cu}_{0.47}\text{As}$ single crystals. We observe four A_g and four B_{3g} phonon modes at 126, 172, 183, 197 cm^{-1} and 101, 139, 173, 226 cm^{-1} , respectively. The results are consistent with the $Ibam$ space group symmetry structure where Fe/Cu atoms form a stripe order. No phonon anomaly is observed cross the magnetic phase transition between 250 to 60 K, suggesting weak electron-phonon and magneto-elastic interaction.

The spectroscopic work at Rutgers was supported by NSF Grant No. DMR-1709161. Sample characterization (WZ) was supported in part by the U.S. Department of Energy, Office of Basic Energy Sciences, Division of Materials Sciences and Engineering under contract No. DE-SC0005463. The crystal growth at Rice was supported by the U.S Department of Energy, Office of Basic Energy Sciences under contract No. DE-SC0012311 and Robert A. Welch Foundation Grant No. C-1839.

* wz131@physics.rutgers.edu

† Current Address: Department of Applied Physics, Northwestern Polytechnical University, Xi'an 710072, China

‡ girsh@physics.rutgers.edu

- [1] G. F. Chen, W. Z. Hu, J. L. Luo, and N. L. Wang, *Phys. Rev. Lett.* **102**, 227004 (2009).
- [2] J. D. Wright, T. Lancaster, I. Franke, A. J. Steele, J. S. Möller, M. J. Pitcher, A. J. Corkett, D. R. Parker, D. G. Free, F. L. Pratt, P. J. Baker, S. J. Clarke, and S. J. Blundell, *Phys. Rev. B* **85**, 054503 (2012).
- [3] A. F. Wang, J. J. Lin, P. Cheng, G. J. Ye, F. Chen, J. Q. Ma, X. F. Lu, B. Lei, X. G. Luo, and X. H. Chen, *Phys. Rev. B* **88**, 094516 (2013).
- [4] G. Tan, Y. Song, R. Zhang, L. Lin, Z. Xu, L. Tian, S. Chi, M. K. Graves-Brook, S. Li, and P. Dai, *Phys. Rev. B* **95**, 054501 (2017).
- [5] C. Ye, W. Ruan, P. Cai, X. Li, A. Wang, X. Chen, and Y. Wang, *Phys. Rev. X* **5**, 021013 (2015).
- [6] Y. Song, Z. Yamani, C. Cao, Y. Li, C. Zhang, J. S. Chen, Q. Huang, H. Wu, J. Tao, Y. Zhu, W. Tian, S. Chi, H. Cao, Y.-B. Huang, M. Dantz, T. Schmitt, R. Yu, A. H. Nevidomskyy, E. Morosan, Q. Si, and P. Dai, *Nat. Commun.* **7**, 13879 (2016).
- [7] C. E. Matt, N. Xu, B. Lv, J. Ma, F. Bisti, J. Park, T. Shang, C. Cao, Y. Song, A. H. Nevidomskyy, P. Dai, L. Patthey, N. C. Plumb, M. Radovic, J. Mesot, and M. Shi, *Phys. Rev. Lett.* **117**, 097001 (2016).
- [8] A. Charnukha, Z. P. Yin, Y. Song, C. D. Cao, P. Dai, K. Haule, G. Kotliar, and D. N. Basov, *Phys. Rev. B* **96**, 195121 (2017).
- [9] M. A. Tanatar, N. Spyrisson, K. Cho, E. C. Blomberg, G. Tan, P. Dai, C. Zhang, and R. Prozorov, *Phys. Rev. B* **85**, 014510 (2012).
- [10] X. Wang, Q. Liu, Y. Lv, Z. Deng, K. Zhao, R. Yu, J. Zhu, and C. Jin, *Science China Physics, Mechanics and Astronomy* **53**, 1199 (2010).
- [11] E. Kroumova, M. Aroyo, J. Perez-Mato, A. Kirov, C. Capillas, S. Ivantchev, and H. Wondratschek, *Phase Transit.* **76**, 155 (2003).
- [12] A. Gozar, *Inelastic Light Scattering in Low Dimensional Quantum Spin Systems*, Ph.D. thesis, University of Illinois at Urbana-Champaign (2004).
- [13] In the set-up, see Fig. 2.1 in [12], Melles Griot Glan-Taylor polarizing prism with better than 10^{-5} extinction ratio was used to clean the laser excitation beam and Karl Lambrecht Corporation broad band polarizing cube with extinction ratio better than 1:500 was used for the analyzer.
- [14] W.-L. Zhang, Z. P. Yin, A. Ignatov, Z. Bukowski, J. Karpinski, A. S. Sefat, H. Ding, P. Richard, and G. Blumberg, *Phys. Rev. B* **93**, 205106 (2016).
- [15] S.-F. Wu, W.-L. Zhang, L. Li, H.-B. Cao, H.-H. Kung, A. S. Sefat, H. Ding, P. Richard, and G. Blumberg, arXiv: 1712.01903 (2017), arXiv:1712.01903.
- [16] M. Klein, "Resonance phenomena," in *Light Scattering in Solids II*, Chap. 2, pp. 45–49.
- [17] Y. J. Um, J. T. Park, B. H. Min, Y. J. Song, Y. S. Kwon, B. Keimer, and M. Le Tacon, *Phys. Rev. B* **85**, 012501 (2012).
- [18] J. Menéndez and M. Cardona, *Phys. Rev. B* **29**, 2051 (1984).